PHYSICAL REVIEW C VOLUME 24, NUMBER 3 SEPTEMBER 1981

Influence of angular momentum on the mass distribution of heavy-ion-induced fission

M. E. Faber
Institut für Kernphysik der Technischen Universität Wien, Schüttelstrasse 115, A-1020 Wien, Austria
(Received 21 March 1980)

The deformation energy surfaces of ^{205}At are calculated at high angular momenta and temperatures using a Woods-Saxon potential and the Strutinsky prescription. By this microscopic calculation it is shown that a qualitative explanation of the increasing width of the mass distribution of heavy-ion-induced fission with angular momentum is possible.

[NUCLEAR REACTIONS ^{205}At; studied mass distribution width of fusion-fission events; dependence on angular momentum; Strutinsky prescription for heated rotating nuclei.]

I. INTRODUCTION

In heavy-ion reactions large angular momenta and highly excited nuclei can be produced. The first step of these reactions is a full damping of the initial relative motion. For the second step there exist two competing possibilities. In the case of complete fusion, a compound nucleus is formed, rotating many times with high angular momentum and subsequently undergoing fission. In the second case of deep inelastic reactions, the contact time is comparatively short and only some nucleons are exchanged. At "low" bombarding energies of about 200 MeV for systems like ^{40}Ar + ^{197}Au the two reaction types are well separated[1-3] and correspond to two well separated regions in a $d^2\sigma/d\theta\, dM$ plot, i.e., in a double differential cross section plot as a function of the center of mass angle θ and of the fragment mass M (see Figs. 2 and 3 of Ref. 2). The complete fusion events are centered around half the mass of the compound nucleus and show no dependence on θ. The deep inelastic events are peaked around the grazing angle and the masses of the target and projectile. At higher energies the separation between both reactions becomes more difficult because of the broadening of the mass distributions.

The aim of this article is to explain the broadening of the mass distribution for the complete fusion events with increasing angular momentum of the compound nucleus and to investigate its deformation energy surface. Experiments[1,3-5] have shown that the width of the mass distribution increases with increasing angular momentum. The calculations of Nix[6] investigate the influence of temperature on mass distributions within the liquid drop model. Moretto[7] calculates the potential energy of a rotating system consisting of two touching liquid drop spheres. From the fact that the potential as a function of mass asymmetry has a minimum at symmetry, the second derivative of which increases with increasing angular momentum, he concludes that the mass distributions for large angular momenta are more sharply peaked around symmetry than the mass distributions for small angular momenta. The Saclay-Orsay group[8,9] explains a broadening of the mass distribution with angular momentum by a new mechanism which is intermediate between compound nucleus formation and deep inelastic reactions. They guess that this new mechanism comes into play when the fission barrier vanishes and they get a mass distribution width increasing abruptly at the corresponding angular momentum.

In this article it will be shown, with the help of a microscopic calculation of the driving force which tends to change the shape parameters of a rotating heated nucleus, that one should expect a smooth increase of the width of the mass distribution with angular momentum. Such potential energy calculations give only qualitative results. For a full dynamic calculation one should know the collective mass parameters. Since there exists no good possibility to calculate these collective masses, it is not possible at the present time to calculate the full dynamics of the system and to get quantitative results. Section II of this article deals with the Strutinsky method for heated, rotating nuclei. In Sec.

 ©1981 The American Physical Society

III the results of such calculations for the nucleus ^{205}At are discussed and compared with the experimental data.

II. THEORY

In principle there exist two possibilities to calculate potential energy surfaces:

(i) First there is the more microscopic treatment by the Hartree-Fock approximation.[10] Using an analytic form of the effective interaction and constraining the static solutions one is able to calculate potential energy curves.

(ii) Second there is the use of a shell model potential together with the shell correction approach of Strutinsky.[11]

Of course, the first method is the more fundamental one. But it has the disadvantage that the computations are even more involved than for the second method. Moreover, the phenomenological effective interactions have difficulties in reproducing accurately the experimentally well known heights of the fission barriers. This article describes calculations by the second method.

The discovery of the importance of deformation effects in the mean field has given rise to a very successful and yet simple parametrization known as the Nilsson model.[12] It has been improved by some corrective terms and is often referred to as the modified harmonic oscillator potential.[13] Several other successful parametrizations are also of common use. The two center harmonic oscillator was developed by the Frankfurt group.[14] Nix and his co-workers[15] have constructed the mean field by convoluting a square well potential with a Yukawa form factor, thus obtaining a reasonable surface diffuseness. The Woods-Saxon potential is used in this article and has been widely developed by the Kiev-Basel-Kopenhagen[16] cooperation.

Analyses based entirely on the single-particle model work reasonably well for moderate quadrupole deformations. For larger deformations, as occur in fission processes, it is essential to incorporate properly the bulk properties of the nucleus by the Strutinsky method[11]; after the parametrization of the shape of the nucleus, the shell model Hamiltonian and finally the Strutinsky method for heated, rotating nuclei will be discussed.

To parametrize the axes of ellipsoidal shapes it is convenient to use the parameters β and γ of Bohr[17] for the axes of the ellipsoid:

$$R_i = R_0[1 + (5/4\pi)^{1/2}\beta\cos(\gamma - i2\pi/3)] \quad . \tag{1}$$

The parameter β describes an elongation, and γ an axial asymmetry of nuclear shapes.

In dimensionless coordinates

$$u = x/R_z, \quad v = y/R_z, \qquad w = z/R_z, \quad \rho^2 = u^2 + v^2 \quad , \tag{2}$$

the equation[16,18]

$$\pi(\rho,w) = \rho^2 - (1 - w^2)(A + Bw^2) = 0 \tag{3}$$

defines an axial symmetric shape with a symmetric neck. For $B = 0$ the shapes are ellipsoidal. The nuclear volume in these coordinates is

$$V = 4\pi/3(A + B/5) \tag{4}$$

and the neck cross section

$$S(w = 0) = \pi A \quad . \tag{5}$$

Instead of the nonillustrative parameters A and B it is useful to generalize[19] the β (and γ) parameters of Bohr. The set of shapes which have the same volume as the ellipsoid parametrized by β, we parametrize also by β. As an additional parameter we introduce the neck parameter r, defined as the ratio of the neck cross section to the cross section of the corresponding ellipsoid (β):

$$r = A/R_\rho^2 = A/(R_u R_v) \quad . \tag{6}$$

This equation together with the volume conservation condition

$$V = (4\pi/3)(A + B/5) = (4\pi/3)R_\rho^2 = (4\pi/3)R_u R_v \tag{7}$$

gives the connection between the $\beta - r$ parametrization and the $A - B$ parametrization. A grid of $\beta - r$ shapes in the x,y,z system is shown in Fig. 1.

Asymmetric dumbbell shapes are defined by the surface[16,18]

$$\pi(\rho,w) = \rho^2 - (1 - w^2)(A + \alpha w + Bw^2) = 0 \quad . \tag{8}$$

Keeping A and B constant and varying α, one gets a set of shapes, which we parametrize by the mass ratio

$$M_r = 2M_1/(M_1 + M_2) \tag{9}$$

of the fragments at both sides of the asymmetric neck. In Fig. 2 a set of such shapes along the liquid

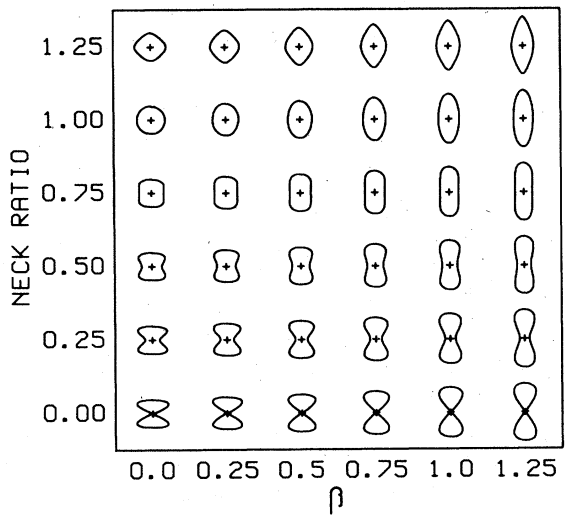

FIG. 1. Axially and reflection symmetric shapes in the $\beta - r$ parametrization.

drop fission valley is shown. The neck ratio r is plotted as an ordinate, and the elongation parameter β (not given in Fig. 2) varies in Fig. 2 according to the relation $\beta = 1.6 - r$. Of course, for the definition of the potential one has to shift the center of the coordinate system to the center of mass

$$w_{\text{c.m.}} = \alpha/(5R_\rho{}^2) \ . \tag{10}$$

In the description of a nucleus by a shell model potential the surface of the nucleus corresponds to the equipotential area, where the potential has half the maximum value $V_0/2$. The central potential of the nucleus is defined by the Woods-Saxon-type potential

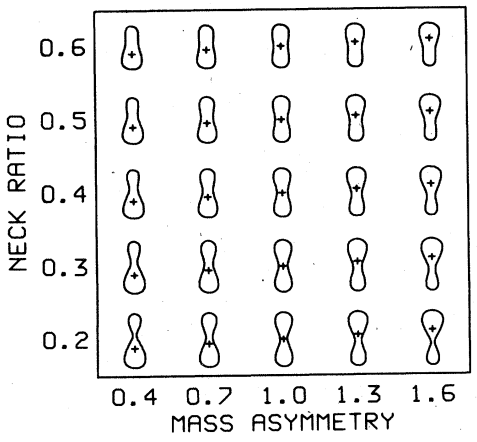

FIG. 2. Mass asymmetric and axially symmetric shapes along the fission valley. The elongation parameter β varies together with the neck ratio r according to $\beta = 1.6 - r$.

$$V^c_{\text{WS}}(\vec{r}) = V_0/\{1 + \exp[1(\vec{r})/a]\} \ . \tag{11}$$

$1(\vec{r})$ is here a length function, defined by[16,20]

$$1(\vec{r}) = \Pi(\rho,z)/|\vec{\nabla}\Pi(\rho,z)|, \ \rho^2 = x^2 + y^2 \ , \tag{12}$$
$$\Pi(r,z) = [\pi(\rho/R_z, z/R_z) - \pi_{\min}]^{1/2} - (-\pi_{\min})^{1/2} \ ,$$

$1(\vec{r}) = 0$ determines the nuclear surface. For a spherical shape we get $1(\vec{r}) = r - R_0$. The central potential is defined in such a way that the thickness of the nuclear surface is constant.

The spin-orbit potential is proportional to the derivative of a Woods-Saxon-type potential

$$V^{\text{so}}(\vec{r}) = -(\kappa/\hbar)\vec{\nabla}V^{\text{so}}_{\text{WS}}[\vec{\sigma}\times\vec{p}]$$
$$= -i\kappa\vec{\sigma}[\vec{\nabla}V^{\text{so}}_{\text{WS}}\times\vec{\nabla}] \ , \tag{13}$$

where $\vec{\sigma}$ is the vector of the Pauli spin matrices.

The shell model Hamiltonian h_0 in the nonrotating coordinate system contains, besides the central potential $V^c_{\text{WS}}(\vec{r})$ and the spin-orbit potential $V^{\text{so}}(\vec{r})$, the kinetic energy operator t and the Coulomb potential $V_{\text{Coul}}(\vec{r})$, approximated by the uniformly charged drop with $Z - 1$ protons

$$h = t + V^c_{\text{WS}}(\vec{r}) + V^{\text{so}}(\vec{r})$$
$$+ \tfrac{1}{2}(1 + \tau_3)V_{\text{Coul}}(\vec{r}) \ . \tag{14}$$

The transformation to the rotating coordinate system can be done by adding the cranking term $-\omega j_x$

$$h_\omega = h_0 - \omega j_x \ , \tag{15}$$

taking Coriolis and centrifugal forces into account. The cranking frequency ω can be interpreted as a Lagrange multipler fixing the x component of the angular momentum operator $\vec{j}$. The parameters of the single-particle Hamiltonian h_ω are listed in Table I.

Solving the Schrödinger equation for protons and

TABLE I. The parameters of the Woods-Saxon potential for the actinide nuclei.

^{240}Pu	Neutrons		Protons	
	V^c_{WS}	$\kappa V^{\text{so}}_{\text{WS}}$	V^c_{WS}	$\kappa V^{\text{so}}_{\text{WS}}$
depth (MeV)	−47.460	−12.000	−62.540	−12.000
radius (fm)	7.730	7.060	7.790	7.060
diffuseness (fm)	0.660	0.550	0.660	0.550
radius of V_{Coul} (fm)	7.017			

neutrons separately one gets the single-particle energies $\epsilon_i^{(\omega)}$ in the rotating coordinate system. It is convenient to do this by a diagonalization of h_ω in a three dimensional harmonic oscillator basis. Only those basis states are taken into account which satisfy

$$E_{\rm def} = (n_x + \tfrac{1}{2})\hbar\omega_x + (n_y + \tfrac{1}{2})\hbar\omega_y + (n_z + \tfrac{1}{2})\hbar\omega_z \leq (N_0 + \tfrac{1}{2})\hbar\omega_0 \ , \tag{16}$$

$N_0 = 10$ and $\hbar\omega_0 = 55\ \text{MeV}/A^{1/3}$. Since the rotational and the time reversal symmetry are broken by the Hamiltonian h_ω there remains only $Q_x = (-1)^{n_x}\Sigma_x$ as a good quantum number. Σ_x is the spin quantum number along the x axis. The dimension of the matrices which have to be diagonalized is of the order 250.

It is very well known[11] that by a simple summation of single-particle energies ϵ_i [or $\epsilon_i^{(\omega)}$] one gets a wrong deformation dependence of the total energy. The total energy has to be renormalized according to the Strutinsky prescription.

We use three kinds of Routhians R, of energies in the rotating system:

(i) First, the independent particle energy

$$R_{\rm IP}(\vec{q},\omega) = \sum_\tau \sum_i \epsilon_i^{(\omega)} n_i^{(\omega)} \ , \tag{17}$$

where $\vec{q}$ represents the set of deformation parameters $\vec{q} = (\beta, r, M_r)$, τ denotes proton or neutron states, and $n_i^{(\omega)}$ are the Hartree-Fock occupation probabilities of the single-particle states.

(ii) Second, the smooth independent particle energy

$$\tilde{R}(\vec{q},\omega) = \sum_\tau \int_{-\infty}^{\tilde{\lambda}_\tau} \epsilon \tilde{g}_\tau(\epsilon) d\epsilon = \sum_\tau \sum_i \epsilon_i^{(\omega)} \tilde{n}_i^{(\omega)} \ , \tag{18}$$

where $\tilde{g}_\tau(\epsilon)$ is the smoothed single-particle density obtained by a Strutinsky smearing[21] of single-particle levels and $\tilde{\lambda}_\tau$ denotes the corresponding Fermi energy.

(iii) Third, the classical energy

$$R_{\rm cl}(\vec{q},\omega) = E_{\rm LDM}(\vec{q}) - \tfrac{1}{2}\mathcal{I}_{\rm rig}(\vec{q})\omega^2 \ , \tag{19}$$

where $\mathcal{I}_{\rm rig}$ denotes the rigid moment of inertia and $E_{\rm LDM}(\vec{q})$ the energy of the nonrotating liquid drop

$$E_{\rm LDM}(\vec{q}) = E_s^0[B_s(\vec{q}) - 1] + E_C^0[B_C(\vec{q}) - 1] \ , \tag{20}$$

and $\vec{q} = (\beta, r, M_r)$ is a vector in the space of deformation parameters. $B_s(\vec{q})$ and $B_C(\vec{q})$ are the surface and Coulomb energies in units of the corresponding energies E_s^0 and E_C^0 for the spherical nucleus. In this article the liquid drop parameters of Pauli and Ledergerber[22] are used. The Strutinsky prescription renormalizes the Routhian R (Ref. 23):

$$R = R_{\rm cl} + \delta R = R_{\rm cl} + (R_{\rm IP} - \tilde{R}) \ .$$

The same procedure can be done for the angular momentum I:

$$I_{\rm IP} = \sum_\tau \sum_i \langle j_x \rangle_{ii}^{(\omega)} n_i^{(\omega)} \ ,$$
$$\tilde{I} = \sum_\tau \sum_i \langle j_x \rangle_{ii}^{(\omega)} \tilde{n}_i^{(\omega)} \ , \tag{21}$$
$$I_{\rm rig} = \omega \mathcal{I}_{\rm rig} \ .$$

Since for the Woods-Saxon potential $I_{\rm rig}$ and $\tilde{I}$ agree very well,[29] the substitution

$$I_{\rm IP} \rightarrow I = I_{\rm rig} + \delta I = I_{\rm rig} + (I_{\rm IP} - \tilde{I}) \tag{22}$$

is possible but not necessary.

The energy in the nonrotating system is then given by

$$E = R + \omega I = E_{\rm RLDM} + \delta E \ ,$$
$$E_{\rm RLDM} = E_{\rm LDM} + \tfrac{1}{2}\mathcal{I}_{\rm rig}\omega^2 \ , \tag{23}$$
$$\delta E = \delta R + \omega \delta I \ .$$

The influence of a thermal excitation of the nucleus can be investigated within the framework of the grand canonical ensemble, which is defined by the statistical operator $\psi = \exp[-(H - \mu N)/T]$. Since the many-particle Hamiltonian $H = \sum_i \epsilon_i^{(\omega)} a_i^\dagger a_i$ is a one-particle operator, the formulas of the independent particle model can be used to calculate the particle number N, the energy E, and the entropy S

$$N = \sum_i n_i, \quad n_i = 1/\{1 + \exp[(\epsilon_i^{(\omega)} - \mu)/T]\} \ ,$$
$$E = \sum_i (\epsilon_i^{(\omega)} + \omega \langle j_x \rangle_{ii}) n_i \ , \tag{24}$$
$$S = -\sum_i [n_i \ln n_i + (1 - n_i)\ln(1 - n_i)] \ .$$

Using the definition of the free energy $F = E - TS$, one obtains from the well known differentials

$$dE = T\,dS - \vec{p}\,d\vec{q} + \mu dN \ ,$$
$$dF = -S\,dT - \vec{p}\,d\vec{q} + \mu dN \ , \tag{25}$$

the Maxwell relations

$$\vec{p} = -\partial E/\partial \vec{q}\,|_{S,N}, \quad \vec{p} = -\partial F/\partial \vec{q}\,|_{T,N} \quad (26)$$

$\vec{p}$ is the driving force, necessary to change the set of deformation parameters $\vec{q} = (\beta, r, M_r)$.

It is not sufficient to do the Strutinsky renormalization for $T = 0$.[24] To get a reduction of shell effects with temperature which is uniform in the whole parameter space,[25] one has to renormalize the level density $g_{sp}(\epsilon) = \sum_i \delta(\epsilon - \epsilon_i^{(\omega)})$ to a liquid drop model density[26]

$$g_{sp} \rightarrow g = g_{LDM} + \delta g = g_{LDM} + (g_{sp} - \tilde{g}) \quad . \quad (27)$$

This can be done by a simple scaling function $s(\epsilon)$ fulfilling

$$\tilde{g}(\epsilon) = \tilde{g}_{sp}[s(\epsilon)] = g_{LDM}(\epsilon) \quad . \quad (28)$$

The scaled single-particle energies $e_i^{(\omega)} = s(\epsilon_i^{(\omega)})$ can be substituted in the above formulas for E and F to get the driving force $\vec{p}$, which determines together with the collective mass parameters the collective path of the nucleus.

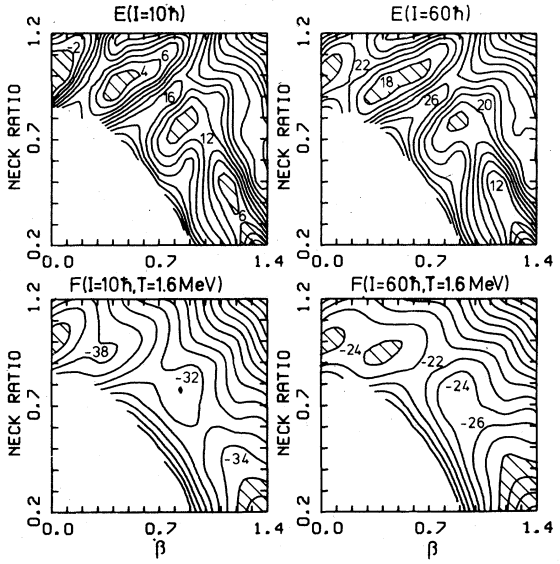

FIG. 3. Deformation energy surfaces of ^{205}At for mass-symmetric and axially symmetric shapes in the $\beta - r$ space: upper left: total energy for $I = 10\hbar$ and $T = 0$; upper right: total energy for $I = 60\hbar$ and $T = 0$; lower left: free energy for $I = 10\hbar$ and $T = 1.6$ MeV; lower right: free energy for $I = 60\hbar$ and $T = 1.6$ MeV.

III. RESULTS

By heavy-ion reactions it is possible to form a nucleus with different angular momentum populations and different excitation energies (temperatures). The influence of angular momentum on the mass distribution width of heavy-ion induced fission of ^{205}At has been studied by experiments of Lebrun *et al.*[1] To make a comparison with these experiments this article shows calculations of potential energy surfaces of ^{205}At.

Calculations in the $\beta - r$ parameter space give a first insight in the behavior of this nucleus. Figure 1 shows a grid of shapes. The elongation parameter β is drawn as the abscissa, the neck ratio r as the ordinate. For ($\beta = 0/r = 1$) one gets the spherical shape, for $r = 1$ the ellipsoidal shape, for $r < 1$ the dumbbell shape, and for $r > 1$ the set of bulged diamondlike shapes. All shapes in the $\beta - r$ space are axially symmetric around the z axis and mirror symmetric to the $x - y$ plane. In Fig. 3 four deformation energy surfaces in the $\beta - r$ space are drawn. Pairing is not included. The energies are in MeV. The distance between the equienergy lines is 2 MeV. The zero point of energy is defined by the energy of the spherical nonrotating liquid drop. The minima of the deformation energy surfaces are hatched. The upper left part of Fig. 3 shows that the ground state of the slowly rotating nucleus is spherical. The second minimum ($\beta \simeq 0.4/r \simeq 0.95$) is higher in energy than the first minimum, the second (symmetric) barrier is higher than the first barrier. At the second saddle ($\beta \simeq 0.85/r \simeq 0.95$) the fission valley starts running through some small "lakes" towards the scission point ($r = 0$). For $I = 60\hbar$ (upper right part of Fig. 3) the second (fission isomeric) minimum is already lower in energy than the first one. The heights of both barriers decrease and the slope of the fission valley increases with angular momentum (see also Figs. 14–16 of Ref. 19).

The influence of an excitation of the nucleus is shown in the lower part of Fig. 3, where the free energy surface for a temperature of 1.6 MeV and a low angular momentum ($I = 10\hbar$) is drawn. An increase of the nuclear temperature enhances the number of statistical particle-hole excitations and decreases the shell structure. At $T = 1.6$ MeV there exist still shell effects giving some wiggles in the equienergy lines. The fission barrier moved now towards a smaller neck ($\beta \simeq 1.0/r \simeq 0.6$). Because of the term $-TS$ in the definition of the free energy $F = E - TS$ the values of the free energy get more negative with increasing T. Only differences of the

free energy are important, since in the framework of the grand canonical ensemble the driving force $\vec{p}$ which tends to change the set of deformation parameters $\vec{q}$ is given by $\vec{p} = -\partial F/\partial \vec{q} \mid_{T,N}$, the gradient of the free energy for constant temperature. The lower right part of Fig. 3 shows the deformation energy surface for a heated ($T = 1.6$ MeV) and fast-rotating ($I = 60\hbar$) nucleus.

For the investigation of fusion-fission events of heavy-ion collisions we follow the picture of a damping of the initial relative motion by an excitation of many nucleons. A mononuclear system is formed. As soon as in the state of slow collective motion thermal equilibrium is reached the potential energy description is possible. The potential energy in the $\beta - r - M_r$ space influences the mass distribution of fusion-fission events. High up in the fission valley the two fragments can still exchange masses. During the fission process this exchange is increasingly inhibited, as the neck between the two fragments narrows and the corresponding collective mass tends to infinity. The important parameter space region for the mass distribution is therefore the region before the mass exchange starts to be frozen.

An investigation of the dependence of the total energy along the fission valley on the mass asymmetry should show the influence of angular momentum on the mass distribution of complete fusion events. In Fig. 4 four free energy surfaces for the temperature $T = 1.6$ MeV are shown. The corresponding shapes are depicted in Fig. 2. The neck ratio r is drawn as the ordinate; r varies from 0.6 to 0.2. The elongation β is changed together with r according to $\beta = 1.6 - r$, as suggested by the direction of the fission valley in the $\beta - r$ plot (Fig. 3). The mass asymmetry $M_r = 2M_1/(M_1 + M_2)$ is plotted as the abscissa. The distance of the equienergy lines is again 2 MeV. For low angular momenta the equienergy lines are narrow parabolas. The driving force acting on a mass asymmetric nucleus (e.g., $r = 0.6/M_r = 0.9$) has a strong component towards symmetry and a very small component along the fission valley. The width of the equipotential parabolas increases slowly for low angular momenta and faster for high angular momenta I. Therefore, the component of the driving force towards symmetric fission decreases. Simultaneously the bottom of the valley descends steeper. The neck narrows faster, since the component of the driving force in the direction of the fission valley increases. An asymmetric quasicompound nucleus at high angular momenta has less tendency and less time to develop towards symmetric fission. The dependence of the driving force $\vec{p}$ on the angular momentum I explains in a simple way the increase of the full width half maximum of the fission mass distribution measured by Lebrun *et al.*[1]

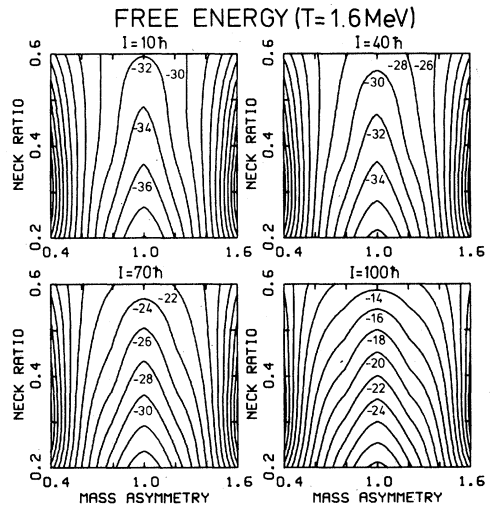

FIG. 4. Free energy surfaces of ^{205}At for mass asymmetric shapes along the fission valley at a temperature of 1.6 MeV. The elongation β varies together with the neck ratio r according to $\beta = 1.6 - r$. The angular momenta $I = 10$, 40, 70, and $100\hbar$ are shown.

The width of the parabolic equienergy lines changes only slightly for small angular momenta and considerably for high angular momenta, in agreement with the experimental results. The reason for this behavior is the difference in the moments of inertia for symmetric and asymmetric compound nuclei. Since asymmetric configurations have larger moments of inertia, their rotational energies do not increase as fast with increasing I as those of symmetric configurations.

Moretto and Schmitt[7] calculate the dependence of the total energy of two touching liquid drop spheres on mass asymmetry and angular momentum within the liquid drop model. They find in agreement with the above calculations that (at the scission point) for sufficiently heavy systems, the potential as a function of mass asymmetry has a minimum at symmetry. The second derivative of this minimum increases with increasing angular momentum. From this fact they conclude that the mass distributions for large angular momenta are more sharply peaked about symmetry than the mass distributions for small angular momenta. But the above discussion shows that it is not sufficient to investigate the potential at the scission point where the mass splitting is already frozen. One has to take into account the

evolution of the system along the fission valley determined by the driving force $\vec{p}$ and the collective masses. If this is done, one arrives at the opposite conclusion from that of Ref. 7.

Gregoire *et al.*[8,9] guess that a new mechanism which is intermediate between deep inelastic reactions and compound nucleus formation is responsible for the increase of the mass distribution width with angular momentum. They guess that this mechanism comes into play when the fission barrier vanishes and get a sudden increase of the width at the corresponding critical angular momentum. The above discussion shows that one can explain the increase of the mass distribution width without assuming a new mechanism, only by investigating the potential energy surface, and that one should expect a smooth increase with angular momentum. This increase is expected to be "quadratic" since the angular momentum enters quadratically in the rotational energy. Of course, the vanishing of the barrier coincides with the increase of the width since the vanishing of the barrier is also connected with a difference between moments of inertia and the dependence of the rotational energy on angular momentum.

For cold actinide nuclei there exist two distinct fission channels,[27] a mass asymmetric channel and a mass symmetric but axially asymmetric channel. A temperature of 1 MeV is sufficient to get rid of the asymmetric mass component.[28] At temperatures of 1.6 MeV the behavior of the nucleus is mainly determined by the liquid drop energy, but as can be seen from Figs. 3 and 4, shell effects may still have some disturbing influence. Since the rotational part of the rotating liquid drop energy is influenced by the moment of inertia the equienergy lines change their shape with increasing angular momentum I. Therefore, the force which tends to press an asymmetric "quasicompound" nucleus versus symmetry decreases with increasing I.

ACKNOWLEDGMENTS

The author is grateful to Professor Amand Faessler for helpful discussions and is grateful for the warm hospitality at IKP-Jülich, where part of the work had been done.

[1]C. Lebrun, F. Hanappe, J. F. Lecolley, F. Lefebvres, C. Ngô, J. Péter, and B. Tamain, Nucl. Phys. A321, 207 (1979).
[2]C. Ngô, J. Péter, B. Tamain, M. Berlanger, and F. Hanappe, Z. Phys. A 283, 161 (1977).
[3]A. Olmi, H.Sann, U. Lynen, V. Metag, S. Bjørnholm, D. Habs, H. J. Specht, R. Bock, A. Gobbi, and H. Stelzer, Proceedings of the 15th International Meeting on Nuclear Physics, Bormio, Italy, 1977 (University of Milan, Milan, Italy, 1978), p. 724.
[4]F. Plasil, D. S. Burnett, H. C. Britt, and S. G. Thompson, Phys. Rev. 142, 696 (1966).
[5]T. Sikkeland, Phys. Lett. 318, 451 (1970).
[6]J. R. Nix, Nucl. Phys. A130, 241 (1969).
[7]L. G. Moretto and R. P. Schmitt, Phys. Rev. C 21, 204 (1980).
[8]C. Gregoire, R. Lucas, C. Ngô, B. Schürmann, and H. Ngô, Nucl. Phys. A361, 443 (1981).
[9]F. Hanappe and B. Borderie, Proceedings of the 17th Winter School on Nuclear Physics, Bierlsko-Biala, Poland, 1980.
[10]P. Quentin and H. Flocard, Ann. Rev. Nucl. Sci. 28, 523 (1978).
[11]V. M. Strutinsky, Nucl. Phys. A95, 420 (1967); A122, 1 (1968).
[12]S. G. Nilsson, K. Dan. Vidensk. Selsk. Mat. Fys. Medd. 29, No. 16 (1955).
[13]G. Andersson, S. E. Larsson, G. Leander, P. Möller, S. G. Nilsson, I. Ragnarsson, S. Åberg, R. Bengtsson, J. Dudek, B. Nerlo-Pomorska, K. Pomorski, and Z. Szymański, Nucl. Phys. A268, 205 (1976).
[14]J. Maruhn and W. Greiner, Z. Phys. 251, 431 (1972).
[15]P. Möller and J. R. Nix, *Proceedings of the Third IAEA Symposium on the Physics and Chemistry of Fission Rochester, 1973* (IAEA, Vienna, 1974), Vol. I.
[16]M. Brack, J. Damgaard, A. S. Jensen, H. C. Pauli, V. M. Strutinsky, and C. Y. Wong, Rev. Mod. Phys. 44, 320 (1972).
[17]A. Bohr, K. Dan. Vidensk. Selsk. Mat. Fys. Medd. 26, No. 14 (1952).
[18]H. C. Pauli, Phys. Rep. 7, 35 (1973).
[19]M. Faber, M. Ploszajczak, and A. Faessler, Nucl. Phys. A326, 129 (1979).
[20]J. Damgaard, H. C. Pauli, V. V. Pashkevich, and V. M. Strutinsky, Nucl. Phys. A135, 432 (1969).
[21]M. Brack and H. C. Pauli, Nucl. Phys. A207, 401 (1973).
[22]H. C. Pauli and T. Ledergerber, Nucl. Phys. A175, 545 (1971).
[23]K. Neergård and V. V. Pashkevich, Phys. Lett. 59B, 218 (1975); K. Neergård, V. V. Pashkevich, and S. Frauendorf, Nucl. Phys. A262, 61 (1976).
[24]A. V. Ignatiuk, I. N. Mikhailov, R. G. Nazmitdinov, B. Nerlo-Pomorska, and K. Pomorski, Phys. Lett. 76B, 543 (1978).
[25]M. E. Faber and M. Ploszajczak, Nucl. Phys. (to be published).
[26]P. A. Gottschalk and T. Ledergerber, Nucl. Phys.

A278, 16 (1977).
[27]A. Gavron, H. C. Britt, P. D. Goldstone, J. B. Wilhelmy, and S. E. Larsson, Phys. Rev. Lett. 38, 1457 (1977).
[28]M. E. Faber, A. Faessler, and M. Ploszajczak, *Proceedings of the Fourth IAEA Symposium on the Physics and Chemistry of Fission, Jülich, 1979* IAEA, Vienna, 1980), Vol. I.
[29]K. Neergård, H. Toki, M. Ploszajczak, and A. Faessler, Nucl. Phys. A287, 48 (1977).